

Received: 21.06.2023

Accepted: 10.11.2023

Research Article

Selective Binding Profiles of Curcumin Derivatives to G-Quadruplex (G4) Structures Found in Human Oncogene Promoters

Hüseyin Saygın Portakal¹

Izmir University of Economics, Genetics and Bioengineering Department

Abstract: G-Quadruplex (G4) structures are special significant DNA topologies formed by accumulation of G-tetrads which are planar structures of four guanine residues interacting with hydrogen bonds through Hoogsten edges around monovalent cations such as potassium (K) or sodium (Na). While these special topologies are mostly observed in telomere regions, they might be found over regulatory regions of the genes such as promoter, enhancer etc. In addition, since that various oncogenes carry G4 structures over their promoters, it's highlighted that G4s have significant role over cancer prognosis through regulation of expression level. To date, binding profiles of curcumin having great antioxidant and anti-inflammatory properties and its derivatives to G4s found in telomere regions and promoter of c-Myc were discovered. As such, to discover selective binding profiles of curcumin derivatives to G4s found in promoters of various oncogenes such as c-Myc, c-KIT, hTERT, RET, VEGF, and PARP1 have quite potential in the drug design for several cancer types. In light of these information, 18 curcumin derivatives from ZINC15 database were docked to related G4 structures. ADME and toxicity properties of all derivatives were analyzed and biological reactivity as well as molecular electrostatic surface potential (MESP) features of totally 4 derivatives (C11, C13, C14, and C15) exhibiting selective binding pattern to certain G4s were analyzed with density functional theory (DFT) method.

Keywords: G-quadruplex, Curcumin, Oncogene, Cancer Prognosis, Cancer Therapeutics, Plant Metabolites

1. Introduction

To date, many biochemical studies have revealed distinct topologies of DNA molecules. G-quadruplexes (G4) are one of the most significant tertiary structures of DNA consist with accumulation of G-tetrad structures which is created via four guanine residues interacting with hydrogen bonds through Hoogsten edges [1], [2]. Main G4 forming sequence has been described as G3+N1-7G3+N1-7G3+N1-7G3+ [3]. While these structures are created as both intra and intermolecular level, the higher thermal stability profiles of G4s comparing to duplex and triplex DNA structures have been revealed with various studies [4]. It's demonstrated that over 300,000 G4 structures are exist in human genome and the most existence frequency is observed in telomere regions in order to inhibit activity of telomerase enzyme [5], [6]. In addition, G4 structures found in

promoter regions of several genes, intron-exon borders, and immunoglobulin recombination genes have been discovered for many years [7]. While these findings show the significance and biological roles of G4s in human metabolism, the discovery of G4s in human oncogene promoters indicate the regulatory role of them over cancer prognosis [8]. For instance, G4 structures in the promoters of c-MYC [9], c-KIT [10], hTERT [11], RET [12], VEGF [13], and PARP1 [14] genes might have a significant role over prognosis of several cancer types through regulation of expression level. Curcumin is a prominent Curcuma longa species sourced herbal chemical compound having great effects over health of human body with antioxidant and anti-inflammatory properties [15]. Furthermore, curcumin is supported as food supplement due to it has a significant effect over brain and heart functions, depression, Alzheimer's

¹ Corresponding Authors

e-mail: saygin.portakal@gmail.com

Hüseyin Saygın Portakal

disease, Arthritis, and cancer [16]. Although curcumin has been approved by FDA as a food coloring agent, the low bioavailability of curcumin is highlighted in literature [17]. This effective polyphenol substance might have a role over the prognosis of aforementioned diseases through targeting the biomolecules acting their signaling pathways. Due to its low bioavailability, distinct derivatives of curcumin have been synthesized and their drug potentials have been analyzed for various diseases [18]. The activity of curcumin derivatives as EGFR and NF- κ B inhibitors, and their inhibitory role over multi-drug resistance Salmonella Typhi's MurC ligase enzyme have been demonstrated with molecular docking based in silico approaches [19], [20]. In addition, that curcumin and its derivatives might recognize G4 structures have been revealed with previous in vitro studies. For instance, Jha and her colleagues have revealed that curcumin and its derivatives could recognize and interact with G4s found in telomere regions of human genome [21]. Moreover, Roy et al. and Pandya et al. have demonstrated the selectively recognition of G4 found in c-Myc promoter by curcumin derivatives, and these compounds might inhibit breast cancer prognosis with two distinct studies [22], [23]. In light of these information, to reveal the selective binding profiles of curcumin derivatives to G4s found in promoters of distinct human oncogenes have a quite potential for further structure based drug design in the treatment of various cancer types. As such, 7 G4 NMR structures found in c-Myc, c-KIT, hTERT, RET, VEGF, and PARP1 promoters were retrieved from Protein Data Bank (PDB), and 18 curcumin derivatives from ZINC15 database were docked to these structures. In order to compare the binding affinities of curcumin derivatives to G4 structures, Braco-19 which is a chemical staining dye and having G4 binding affinity was analyzed with same computational strategy. Once to complete the docking study, ADME properties of the compounds were analyzed by considering Lipinski's rule of five, their toxicities and lethal doses (LD50) were predicted with various in silico applications. Finally, bioreactivities and molecular surface electrostatic potentials of of best curcumin derivatives exhibiting selective binding pattern as well as Braco-19 were analyzed with density functional theory (DFT) methods.

2. Computational Method

2.1. Molecular Docking

G4 structures found in promoter regions of c-Myc, c-KIT, hTERT, RET, VEGF, and PARP1 were retrieved from PDB Data Bank (PDB) with PDB IDs: 1XAV, 2KYP, 2KZE, 2L88, 2M27, and 6AC7, respectively. Retrieved .pdb files were prepared for molecular docking through Dock Prep package of Chimer 1.16 by removing monovalent cations, water molecules, adding partial charges, hydrogen atoms, and side chain replacing with the rotamer library of Dunbrack 2010 [24]. Prepared DNA structures were imported to PyRx virtual screening tool in .pdbqt format [25]. Curcumin Library including 18 curcumin derivatives was created by retrieving the ligands from ZINC15 database. The library was imported to PyRx and prepared by energy minimization module. Minimized compounds were blindly docked to DNA structures with AutoDock Vina package of the software and .csv files including binding affinity, rmsd/lb, and rmsd/ub values were exported [26]. Once to analyze the binding affinities, the interactions between DNA molecules and docked compounds' mode having 0 rmsd/lb, and rmsd/ub values were investigated with Discovery Studio.

2.2. Validation Study

Braco-19 is a chemical compound with G4 binding affinity. Furthermore, the compound is frequently used as G4 staining and stabilizing molecule in biotechnological researches. As such, validation of the study was carried out by following molecular docking strategy with Braco-19 and related G4 structures. Considering the binding affinity and physicochemical properties of Braco-19, the efficiencies of the curcumin derivatives were discussed.

2.3. ADME and Toxicity Analysis

A convenient drug molecule should have proper physicochemical properties in order to have absorption, distribution, metabolism, and excretion (ADME) features to reach accurate region of host body with quite efficiency. While ADME properties of a drug might be analyzed with various in silico techniques, Lipinski's rule of five points that an ideal drug should have less than 500 kDA molecular weight, less than 10 hydrogen bond acceptors, less than 5 hydrogen bond donors, and

Hüseyin Saygın Portakal

less than 5 CLogP (water partition coefficient) [27]. These parameters might be analyzed with investigation of absorption, distribution, metabolism, and excretion (ADME) properties of the compounds. As such, ADME analysis of curcumin derivatives as well as Braco-19 was carried out with swissADME online server and the Lipinski's rule of five parameters were revealed [28]. In addition, possible toxicities and LD50 values of the compounds were predicted with both ProTox II online server [29] and OSIRIS Property Explorer tool [30].

2.4. Geometry Optimization, DFT Calculation, and Molecular Electrostatic Surface Potential (MESP) Analysis

Once to reveal curcumin derivatives exhibiting selective binding profiles to certain G4 structures (C11, C13, C14, and C15), the molecular geometries of them and Braco-19 were minimized with Gaussian 09 software following B3LYP/6-31G basis set [31] [32]. In order to analyze their biological reactivities, highest occupied molecular orbital (HOMO) and lowest unoccupied molecular orbital (LUMO) energy levels were analyzed in GaussView. Biological reactivity profiles of the compounds were analyzed with calculation of electron affinity ($A = -E_{LUMO}$), ionization potential ($I = -E_{HOMO}$), energy gap ($E_{gap} = E_{LUMO} - E_{HOMO}$), hardness ($\eta = (I-A)/2$), softness ($S = 1/\eta$), chemical potential ($\mu = -(I+A)/2$), and electrophilicity ($\omega = \mu^2/2\eta$) features of the substances [33]. Once to complete DFT analysis, molecular electrostatic surface potential (MESP) features of the geometrically minimized compounds were analyzed with Avagadro molecular visualization software [34].

3. Results and discussion

While oncogenes are responsible for cancer prognosis through mutations or increased expression level, various oncogenes may lead to progression of certain cancer types. For instance deregulation over c-Myc oncogene might cause colon, lung, breast, stomach, and cervix cancer [35], as a tyrosine kinase receptor the deregulation over c-KIT may serve to acute myeloid leukemia and gastrointestinal stromal cancer [36], vascular endothelial growth factor (VEGF) triggers blood vessel formation and its deregulation have

significant role over several cancer prognosis especially in breast cancer [37], overexpression of Poly[ADP-ribose] polymerase 1 (PARP1) is observed in various cancer types such as breast, colon, and gastric cancer [38], deregulation of human telomerase reverse transcriptase (hTERT) is assessed as having quite significant role over almost all cancer types [39], and as another tyrosine kinase receptor RET proto-oncogene might act a role over medullary thyroid cancer prognosis [40]. Considering such those knowledge, designing novel therapeutics targeting certain biomolecule structures having a role in cancer progression is one of the main efforts of medicinal chemistry and biotechnology research areas in order to develop specialized treatment approaches. Furthermore, due to that expression level of these genes are regulated by G4 structures found in their promoter regions, to reveal selective binding profiles of curcumin derivatives to these topologies opens a new gate into structure based drug design studies.

In this scope, totally 18 curcumin derivatives and 6 G4 structures were retrieved from ZINC15 and PDB databases, respectively. Retrieved ligands were blindly docked to crystal structures of DNA molecules. In addition, in order to validate the study, Braco-19 having a binding affinity to G4s were docked to structures by following the same strategy [41]. Data demonstrating the computed binding affinities of the compounds for each G4 are listed Table 1. The findings have demonstrated that C11 has highest binding affinity to G4 in PARP1 promoter, C13 and C14 have highest affinity to G4 in VEGF promoter, and C15 has highest binding affinity to G4 in RET promoter comparing the other G4 structures. Since that binding profiles of curcumin derivatives had been previously demonstrated, G4 structure in c-Myc promoter was ignored in the evaluation. The observed affinity values of Braco-19 to all G4s proves the binding profile of the ligand for these prominent DNA topologies and demonstrates the efficiency of the strategy which has been developed during the study. The chemical structures of curcumin derivatives having selective binding profiles to related G4 structures are demonstrated in Figure 1. The chemical structures of the compounds have pointed that C11, C13, and C14 have only stereochemistry differences and the structures of the compounds might be a scaffold for drug design

Hüseyin Saygın Portakal

studies. In addition the interactions created in ligand-DNA interfaces of the derivatives as well as Braco-19 are demonstrated in Figure 2.

ADME properties defines whether the features of a chemical compound are suitable to be a drug molecule in the treatment of diseases [42]. In particular, according to Lipinski's rule of five a molecule might be assessed as an efficient drug molecule if it has less than 500 kDa molecular weight, less than 10 hydrogen bond acceptors, less than 5 hydrogen bond donors, and less than 5 CLogP (water partition coefficient) [27]. Considering such these information, ADME properties of all curcumin derivatives as well as Braco-19 were investigated with swissADME

online server and the features of compounds in the scope of Lipinski's rule of five were listed in Table 2. The findings have demonstrated that although first six curcumin derivatives are following Lipinski's rule of five, the compounds having selective binding profiles which are C11, C13, C14, and C15 obey only one parameter. In addition, apart from its molecular weight, Braco-19 follows Lipinski's rule of five. As such, it's assessed that these curcumin derivatives having selective binding pattern to G4s found in oncogene promoters should be designed with medicinal chemistry approaches in order to achieve an ideal drug with ideal ADME properties.

Table 1. Binding affinity values of curcumin derivatives and Braco-19 to G4s found in certain oncogene promoters in kcal/mole unit.

| Curcumin Derivatives | Oncogene | | | | | |
|---------------------------|----------|-------|-------|------|------|-------|
| | c-Myc | c-KIT | hTERT | RET | VEGF | PARP1 |
| C1 (ZINC000000899824) | -6.9 | -6.0 | -6.1 | -6.3 | -6.8 | -6.7 |
| C2 (ZINC000014948330) | -5.4 | -4.7 | -5.1 | -5.7 | -5.0 | -7.0 |
| C3 (ZINC000016527488) | -6.3 | -6.1 | -5.7 | -5.6 | -6.5 | -7.4 |
| C4 (ZINC000019816066) | -7.9 | -6.9 | -6.3 | -6.9 | -7.3 | -6.7 |
| C5 (ZINC000085926636) | -5.5 | -5.5 | -5.7 | -6.5 | -6.8 | -7.5 |
| C6 (ZINC000100067274) | -7.1 | -6.7 | -6.4 | -6.8 | -6.9 | -7.0 |
| C7 (ZINC000150366575) | -8.0 | -6.9 | -5.3 | -7.5 | -7.0 | -8.3 |
| C8 (ZINC000150366578) | -7.8 | -7.2 | -6.7 | -7.9 | -8.3 | -7.1 |
| C9 (ZINC000150366582) | -8.0 | -6.3 | -6.5 | -7.4 | -8.1 | -7.7 |
| C10 (ZINC000150366588) | -7.8 | -7.0 | -6.8 | -7.1 | -7.4 | -8.0 |
| C11 (ZINC000150368101) | -7.9 | -7.6 | -7.4 | -8.2 | -6.1 | -8.4 |
| C12 (ZINC000150368109) | -8.3 | -7.2 | -6.0 | -7.5 | -8.2 | -7.7 |
| C13 (ZINC000150368115) | -8.2 | -6.4 | -7.7 | -8.1 | -8.2 | -7.9 |
| C14 (ZINC000150368122) | -8.6 | -6.0 | -7.4 | -6.7 | -8.4 | -6.7 |
| C15 (ZINC000150368128) | -8.1 | -7.1 | -6.7 | -8.4 | -7.8 | -7.2 |
| C16 (ZINC000150368132) | -8.3 | -7.2 | -5.7 | -6.5 | -7.6 | -6.5 |
| C17 (ZINC000150368137) | -8.1 | -6.9 | -5.7 | -6.8 | -6.9 | -6.6 |
| C18 | -7.0 | -7.3 | -7.4 | -8.0 | -7.1 | -7.0 |

(ZINC000150368142)

Braco-19

-8.5

-7.5

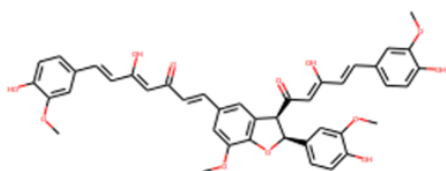
-8.0

-7.4

-8.0

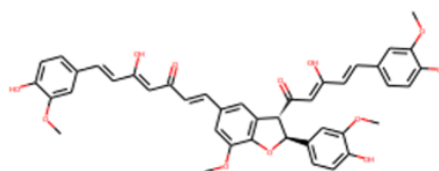
-7.8

Chemical Structures of Curcumin Derivatives



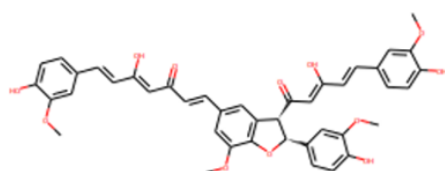
C11

(ZINC000150368101)



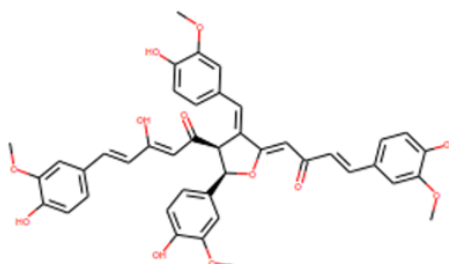
C13

(ZINC000150368115)



C14

(ZINC000150368122)



C15

(ZINC000150368128)

Figure 1. Chemical Structures of curcumin derivatives having selective binding profiles to G4 structures found in certain oncogene promoters.

Once to complete ADME analysis, possible toxicities and lethal dose for 50% of the population (LD50) values of curcumin derivatives and Braco-19 were predicted with both ProTox II online server and OSIRIS Property Explorer tool. The data demonstrating the toxicity features and LD50 values of the chemical compounds are listed in Table 3. Considering the results, it's observed that any curcumin derivatives do not exhibit any kind of toxicity in the human body, yet Braco-19 might have possible mutagenicity, tumorigenicity, and reproductive effect. Thus, as G4 binding agent curcumin derivatives exhibits no toxicity contrary to Braco-19. In addition, LD50 values define the concentration of a compound that might be lethal for 50% of the population [43]. That is, LD50 values are strong indicator in toxicity analysis of such those compounds. In light of the data LD50 values of C11, C13, C14, and C15 were predicted as 1500 mg/kg. In addition LD50 value of Braco-

19 was predicted as 695 mg/kg, and of cisplatin which is an anticancer agent and frequently used as model drug in cancer researches was defined as 13.5 mg/kg in literature [44]. Furthermore, in order to enhance LD50 values of cisplatin, studies aiming to design novel cisplatin analogues had been carried out, previously [45]. Therefore it's revealed that curcumin derivatives with selective binding profiles to distinct G4 structures are less toxic than Braco-19 and cisplatin for human body.

Once to complete ADME and toxicity analysis, biological reactivity of C11, C13, C14, C15, and Braco-19 were analyzed with DFT based method. As such, geometries of the chemical compounds were minimized with Gaussian 09 software and energy levels of HOMO and LUMO of each compound were revealed. While HOMO energy level shows electron donating tendency, LUMO shows electron accepting tendency. That is, these levels have significant role for interactions with

Hüseyin Saygın Portakal

molecules through electron transferring [46]. Furthermore, energy gap (Egap), electron affinity (A), ionization potential (I), chemical potential (μ), softness (S), hardness (η), electrophilicity (ω), and electronegativity (X) properties of a chemical

compound might be computed with the EHOMO and ELUMO values. Such those properties are the main parameters indicating biological reactivity profiles of chemical compounds [33].

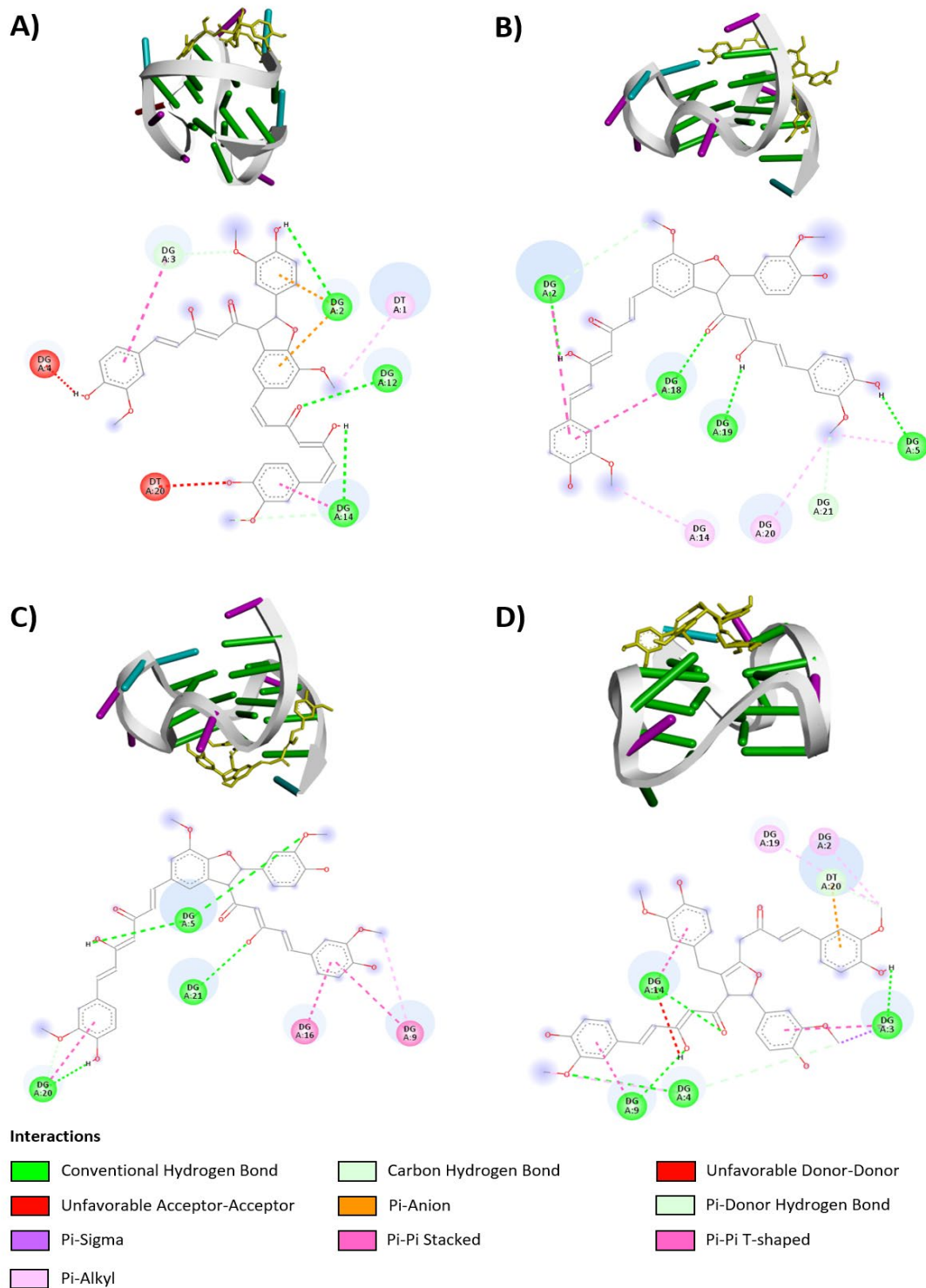


Figure 2. 3D and 2D illustrations of interactions between curcumin derivatives and PDB files; A) C11-6AC7, B) C13-2M27, C) C14-2M27, and D) C15-2L88.

Hüseyin Saygın Portakal

Table 2. ADME profiles of curcumin derivatives and Braco-19 considering Lipinski's rule of five parameters.

| Curcumin Derivatives | Lipinski's Rule of Five | | | |
|---------------------------|-------------------------|------------------|-------------|----------|
| | <10 H-bond acceptors | <5 H-bond donors | <500 kDa Mw | <5 ClogP |
| C1 (ZINC000000899824) | Yes | Yes | Yes | Yes |
| C2 (ZINC000014948330) | Yes | Yes | Yes | Yes |
| C3 (ZINC000016527488) | Yes | Yes | Yes | Yes |
| C4 (ZINC000019816066) | Yes | Yes | Yes | Yes |
| C5 (ZINC000085926636) | Yes | Yes | Yes | Yes |
| C6 (ZINC000100067274) | Yes | Yes | Yes | Yes |
| C7 (ZINC000150366575) | No | Yes | No | Yes |
| C8 (ZINC000150366578) | No | Yes | No | Yes |
| C9 (ZINC000150366582) | No | Yes | No | Yes |
| C10 (ZINC000150366588) | No | Yes | No | Yes |
| C11 (ZINC000150368101) | No | Yes | No | No |
| C12 (ZINC000150368109) | No | Yes | No | No |
| C13 (ZINC000150368115) | No | Yes | No | No |
| C14 (ZINC000150368122) | No | Yes | No | No |
| C15 (ZINC000150368128) | No | Yes | No | No |
| C16 (ZINC000150368132) | No | Yes | No | No |
| C17 (ZINC000150368137) | No | Yes | No | No |
| C18 (ZINC000150368142) | No | Yes | No | No |
| Braco-19 | Yes | Yes | No | Yes |

It's previously referred that low chemical potential, hardness, electrophilicity, ionization potential, ad high energy gap, electron affinity, electronegativity, softness provide high biological reactivity to the chemical compounds [47]. Results have demonstrated that while biological reactivities of all compounds exhibit similarity, Braco-19 has the highest reactivity among the all substances (Table 4). While the findings were parallel with ADME results, that curcumin derivatives with

selective binding profiles should be evolved to be ideal drugs having sufficient biological reactivity. Ultimately, molecular electrostatic potential (MESP) map of the curcumin derivatives were analyzed with Avagadro software (Figure 3). Considering MESP map the electron density, electrophilic and nucleophilic regions, and charge distribution of each compounds might be analyzed [48]. While blue regions indicate low density of electrons, red regions show high electron content.

Hüseyin Saygın Portakal

Table 3. Predicted toxicity properties and LD50 values of curcumin derivatives and Braco-19.

| Curcumin Derivatives | Toxicity Profiles | | | | |
|---------------------------|-------------------|----------------|-----------------|---------------------|--------------|
| | Mutagenicity | Tumorigenicity | Irritant Effect | Reproductive Effect | LD50 (mg/kg) |
| C1 (ZINC000000899824) | No | No | No | No | 2000 |
| C2 (ZINC000014948330) | No | No | No | No | 410 |
| C3 (ZINC000016527488) | No | No | No | No | 1000 |
| C4 (ZINC000019816066) | No | No | No | No | 1560 |
| C5 (ZINC000085926636) | No | No | No | No | 1000 |
| C6 (ZINC000100067274) | No | No | No | No | 4000 |
| C7 (ZINC000150366575) | No | No | No | No | 1500 |
| C8 (ZINC000150366578) | No | No | No | No | 1500 |
| C9 (ZINC000150366582) | No | No | No | No | 1500 |
| C10 (ZINC000150366588) | No | No | No | No | 1500 |
| C11 (ZINC000150368101) | No | No | No | No | 1500 |
| C12 (ZINC000150368109) | No | No | No | No | 1500 |
| C13 (ZINC000150368115) | No | No | No | No | 1500 |
| C14 (ZINC000150368122) | No | No | No | No | 1500 |
| C15 (ZINC000150368128) | No | No | No | No | 1500 |
| C16 (ZINC000150368132) | No | No | No | No | 1500 |
| C17 (ZINC000150368137) | No | No | No | No | 1500 |
| C18 (ZINC000150368142) | No | No | No | No | 1500 |
| Braco-19 | Yes | Yes | No | Yes | 695 |

Table 4. The values pointing bioreactivity profiles of the curcumin derivatives having selective binding pattern and Braco-19

| Ligand | DFT Analysis | | | | | | | | | |
|----------|--------------|----------|-----------------|-----------------|-----------------------------------|------------------|------------------|--------------|---------------|------------------------|
| | HOMO | LUMO | $I = -E_{HOMO}$ | $A = -E_{LUMO}$ | $E_{gap} = (E_{LUMO} - E_{HOMO})$ | $\mu = -(I+A)/2$ | $\eta = (I-A)/2$ | $S = 1/\eta$ | $X = (I+A)/2$ | $\omega = \mu^2/2\eta$ |
| C11 | -0.18581 | -0.08896 | 0.18581 | 0.08896 | 0.09685 | -0.137385 | 0.048425 | 20.650490 | 0.137385 | 0.194885 |
| C13 | -0.19279 | -0.08561 | 0.19279 | 0.08561 | 0.10718 | -0.1392 | 0.05359 | 18.660198 | 0.1392 | 0.180786 |
| C14 | -0.18710 | -0.09111 | 0.18710 | 0.09111 | 0.09599 | -0.139105 | 0.047995 | 20.835504 | 0.139105 | 0.201586 |
| C15 | -0.18909 | -0.09863 | 0.18909 | 0.09863 | 0.09046 | -0.14386 | 0.04523 | 22.109220 | 0.14386 | 0.228783 |
| Braco-19 | -0.17047 | -0.06287 | 0.17047 | 0.06287 | 0.1076 | -0.11667 | 0.0538 | 18.584361 | 0.11667 | 0.126505 |

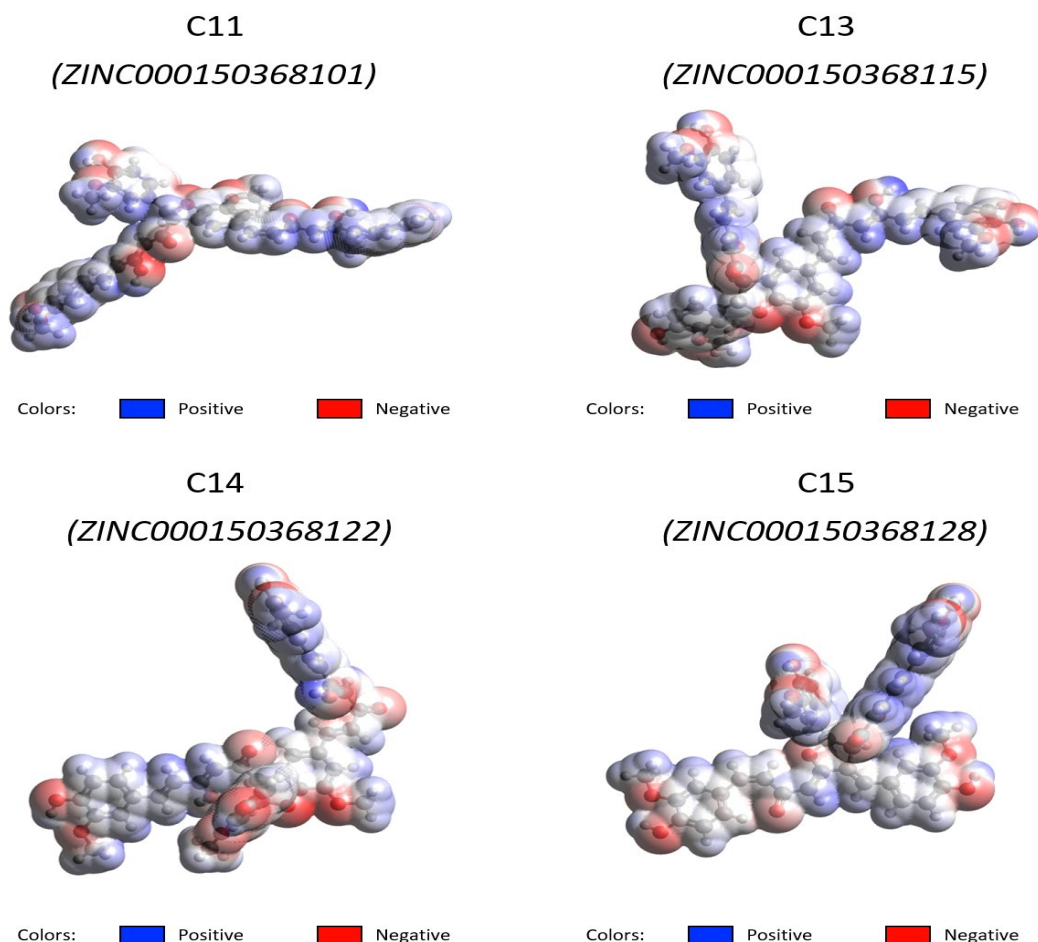


Figure 3. Molecular electrostatic potential (MESP) map of curcumin derivatives having selective binding profiles to G4s found in certain oncogene promoters.

4. Conclusions

G4s are one of the most prominent nucleic acid secondary structures having essential roles in cellular metabolism. In particular, G4s found in oncogene promoters may lead to various cancer prognosis through regulating the expression level. Curcumin is an herbal product having antioxidant and anti-inflammatory activity. In addition, the sufficient binding affinity of curcumin and its derivatives to G4s found in c-Myc promoter and telomere regions were demonstrated previously. Despite these facts that any data pointing selective binding profile of curcumin derivatives to G4s found in oncogene promoters had not been published, to date. In this study, 18 curcumin derivatives from ZINC15 database were retrieved and docked to G4 structures found in promoters of c-Myc, c-KIT, hTERT, RET, VEGF, and PARP1 oncogenes. The binding affinity results have demonstrated that C11, C13, C14, and C15 have selective binding pattern to distinct G4s. Furthermore, ADME properties and possible toxicities of the curcumin derivatives were investigated with various in silico techniques. Once

to reveal selective curcumin derivatives their biological reactivities and molecular electrostatic potential (MESP) maps were revealed with DFT based methods. Findings put forward that even though C11, C13, C14, and C15 have selective binding profiles to certain G4 structures and have low toxicity for human body, yet their ADME properties and biological reactivity profiles are inadequate to be used as a drug molecule in the treatment of related cancer types. However, novel drug molecules designed by referencing the chemical structures of the derivatives as scaffold might be developed subsequently and these findings might keep light to further researches in this area.

References

- [1] Z. Y. Sun, X. N. Wang, S. Q. Cheng, X. X. Su, and T. M. Ou, Developing novel G-quadruplex ligands: From interaction with nucleic acids to interfering with nucleic acid-protein interaction, *Molecules*, 24 (2019) 369-398.

Hüseyin Saygın Portakal

- [2] Z. Zhang, J. Dai, E. Veliath, R. A. Jones, and D. Yang, Structure of a two-G-tetrad intramolecular G-quadruplex formed by variant human telomeric sequence in K⁺ solution: Insights into the interconversion of human telomeric G-quadruplex structures, *Nucleic Acids Res.*, 38 (2009) 1009–1021.
- [3] S. Q. Mao et al., DNA G-quadruplex structures mold the DNA methylome, *Nat. Struct. Mol. Biol.*, 25 (2018) 951–957.
- [4] T. Fujimoto, D. Miyoshi, H. Tateishi-Karimata, and N. Sugimoto, Thermal stability and hydration state of DNA G-quadruplex regulated by loop regions, *Nucleic Acids Symp. Ser.*, 53 (2009) 237–238.
- [5] Y. Ding, A. M. Fleming, and C. J. Burrows, Case studies on potential G-quadruplex-forming sequences from the bacterial orders Deinococcales and Thermales derived from a survey of published genomes, *Sci. Rep.*, 8 (2018) 1–11.
- [6] T. M. Bryan, G-quadruplexes at telomeres: Friend or foe?, *Molecules*, 25 (2020) 1-22.
- [7] D. Varshney, J. Spiegel, K. Zyner, D. Tannahill, and S. Balasubramanian, The regulation and functions of DNA and RNA G-quadruplexes, *Nat. Rev. Mol. Cell Biol.*, 21 (2020) 459–474.
- [8] N. Kosiol, S. Juranek, P. Brossart, A. Heine, and K. Paeschke, G-quadruplexes: a promising target for cancer therapy, *Mol. Cancer*, 20 (2021) 1–18.
- [9] R. I. Mathad, E. Hatzakis, J. Dai, and D. Yang, C-MYC promoter G-quadruplex formed at the 5'-end of NHE III 1 element: Insights into biological relevance and parallel-stranded G-quadruplex stability, *Nucleic Acids Res.*, 39 (2011) 9023–9033.
- [10] S. Mazzini et al., Stabilization of c-KIT G-quadruplex DNA structures by the RNA polymerase I inhibitors BMH-21 and BA-41, *Int. J. Mol. Sci.*, 20 (2019) 1–17.
- [11] A. V. Pavlova et al., G-Quadruplex Formed by the Promoter Region of the hTERT Gene: Structure-Driven Effects on DNA Mismatch Repair Functions, *Biomedicines*, 10 (2022) 1871-1892.
- [12] X. Tong, W. Lan, X. Zhang, H. Wu, M. Liu, and C. Cao, Solution structure of all parallel G-quadruplex formed by the oncogene RET promoter sequence, *Nucleic Acids Res.*, 39 (2011) 6753–6763.
- [13] P. Agrawal, E. Hatzakis, K. Guo, M. Carver, and D. Yang, Solution structure of the major G-quadruplex formed in the human VEGF promoter in K⁺: Insights into loop interactions of the parallel G-quadruplexes, *Nucleic Acids Res.*, 41 (2013) 10584–10592.
- [14] A. D. Edwards, J. C. Marecki, A. K. Byrd, J. Gao, and K. D. Raney, G-Quadruplex loops regulate PARP-1 enzymatic activation, *Nucleic Acids Res.*, 49 (2021) 416–431.
- [15] S. J. Hewlings and D. S. Kalman, Curcumin: A review of its effects on human health, *Foods*, 6 (2017) 1–11.
- [16] A. Rahmani, M. Alsahli, S. Aly, M. Khan, and Y. Aldebasi, Role of Curcumin in Disease Prevention and Treatment, *Adv. Biomed. Res.*, 7 (2018) 38-47.
- [17] A. L. Lopresti, The problem of curcumin and its bioavailability: Could its gastrointestinal influence contribute to its overall health-enhancing effects?, *Adv. Nutr.*, 9 (2018) 41–50.
- [18] S. I. Sohn et al., Biomedical applications and bioavailability of curcumin—an updated overview, *Pharmaceutics*, 13 (2021) 1–33.
- [19] M. E. M. Saeed et al., In Silico and In Vitro Screening of 50 Curcumin Compounds as EGFR and NF-κB Inhibitors, *Int. J. Mol. Sci.*, 23 (2022) 3966–3984.
- [20] A. Roy et al., MurC Ligase of multi-drug resistant *Salmonella Typhi* can be inhibited by novel Curcumin derivative: Evidence from molecular docking and dynamics simulations, *IJBCB*, 151 (2022) 106279–106288.
- [21] R. Debroy and S. Ramaiah, Targeting human telomeric G-quadruplex DNA with curcumin and its synthesized analogues under molecular crowding conditions, *RSC Adv.*, 6 (2016) 7474–7487.
- [22] A. Roy et al., Curcumin arrests G-quadruplex in the nuclear hyper-sensitive III1 element of c-MYC oncogene leading to apoptosis in metastatic breast cancer cells, *J. Biomol. Struct. Dyn.*, 40 (2022) 10203–10219.

Hüseyin Saygın Portakal

- [23] N. Pandya et al., Curcumin analogs exhibit anti-cancer activity by selectively targeting G-quadruplex forming c-myc promoter sequence, *Biochimie*, 180 (2021) 205–221.
- [24] E. F. Pettersen et al., UCSF Chimera - A visualization system for exploratory research and analysis, *J. Comput. Chem.*, 25 (2004) 1605–1612.
- [25] S. Dallakyan, A. Olson, *Small-Molecule Library Screening by Docking with PyRx*, NY: Springer New York, U.S.A, 2015, 243-250.
- [26] O. Trott, A. J. Olson, AutoDock Vina: improving the speed and accuracy of docking with a new scoring function, efficient optimization and multithreading, *J. Comput. Chem.* 17 (2011) 295-304.
- [27] L. Z. Benet, C. M. Hosey, O. Ursu, and T. I. Oprea, BDDCS, the Rule of 5 and drugability, *Adv. Drug Deliv. Rev.*, 101 (2016) 89–98.
- [28] A. Daina, O. Michielin, and V. Zoete, SwissADME: A free web tool to evaluate pharmacokinetics, drug-likeness and medicinal chemistry friendliness of small molecules, *Sci. Rep.*, 7 (2017) 1–13.
- [29] P. Banerjee, A. O. Eckert, A. K. Schrey, and R. Preissner, ProTox-II: A webserver for the prediction of toxicity of chemicals, *Nucleic Acids Res.*, 46 (2018) 257–26.
- [30] <https://www.organic-chemistry.org/prog/peo/>, January 2017, Accessed: 06.12.2022.
- [31] J. Tirado-rives and W. L. Jorgensen, Performance of B3LYP Density Functional Methods for a Large Set of Organic Molecules, 4 (2008) 297–306.
- [32] M. J. Frisch, G. W. Trucks, H. B. Schlegel, G. E. Scuseria, M. A. Robb, J. R. Cheeseman, G. Scalmani, V. Barone, G. A. Petersson, H. Nakatsuji, X. Li, M. Caricato, A. Marenich, J. Bloino, B. G. Janesko, R. Gomperts, B. Mennucci, H. P. Hratchian, J. V. Ortiz, A. F. Izmaylov, J. L. Sonnenberg, D. Williams-Young, F. Ding, F. Lipparini, F. Egidi, J. Goings, B. Peng, A. Petrone, T. Henderson, D. Ranasinghe, V. G. Zakrzewski, J. Gao, N. Rega, G. Zheng, W. Liang, M. Hada, M. Ehara, K. Toyota, R. Fukuda, J. Hasegawa, M. Ishida, T. Nakajima, Y. Honda, O. Kitao, H. Nakai, T. Vreven, K. Throssell, J. A. Montgomery, Jr., J. E. Peralta, F. Ogliaro, M. Bearpark, J. J. Heyd, E. Brothers, K. N. Kudin, V. N. Staroverov, T. Keith, R. Kobayashi, J. Normand, K. Raghavachari, A. Rendell, J. C. Burant, S. S. Iyengar, J. Tomasi, M. Cossi, J. M. Millam, M. Klene, C. Adamo, R. Cammi, J. W. Ochterski, R. L. Martin, K. Morokuma, O. Farkas, J. B. Foresman, and D. J. Fox, *Gaussian 09*, Inc., Wallingford CT, 2009.
- [33] M. A. Raza, U. Farwa, F. Ishaque, A. G. Al-Sehemi, Designing of Thiazolidinones against Chicken Pox, and Hepatitis Viruses: A Computational Approach, *Comput. Biol. Chem.*, 103 (2023) 1–15.
- [34] M. D. Hanwell, D. E. Curtis, D. C. Lonie, T. Vandermeersch, E. Zurek, and G. R. Hutchison, Avogadro: An advanced semantic chemical editor, visualization, and analysis platform, *J. Cheminform.*, 4 (2012) 1-17.
- [35] D. M. Miller, S. D. Thomas, A. Islam, D. Muench, and K. Sedoris, c-Myc and cancer metabolism, *Clin. Cancer Res.*, 18 (2012) 5546–5553.
- [36] A. F. Abdel-Magid, The Potential of c-KIT Kinase inhibitors in Cancer Treatment, *ACS Med. Chem. Lett.*, 12 (2021) 1191–1192.
- [37] P. Carmeliet, VEGF as a key mediator of angiogenesis in cancer, *Oncology*, 69 (2005) 4–10.
- [38] L. Wang et al., PARP1 in carcinomas and PARP1 inhibitors as antineoplastic drugs, *Int. J. Mol. Sci.*, 18 (2017) 1–16.
- [39] K. Wang et al., The prognostic significance of hTERT overexpression in cancers, *Medicine (Baltimore)*, 97 (2018) 11794-11802.
- [40] M. Takahashi, K. Kawai, and N. Asai, Roles of the RET Proto-oncogene in Cancer and Development, *JMA J.*, 3 (2020) 175–181.
- [41] A. M. Burger et al., The G-quadruplex-interactive molecule BRACO-19 inhibits tumor growth, consistent with telomere targeting and interference with telomerase function, *Cancer Res.*, 65 (2005) 1489–1496.
- [42] S. Q. Pantaleão, P. O. Fernandes, J. E. Gonçalves, V. G. Maltarollo, and K. M. Honorio, Recent Advances in the Prediction of Pharmacokinetics Properties in Drug

Hüseyin Saygın Portakal

- Design Studies: A Review, *ChemMedChem*, 17 (2022) 1-13.
- [43] G. Zbinden and M. Flury-Roversi, Significance of the LD50-test for the toxicological evaluation of chemical substances, *Arch. Toxicol.*, 47 (1981) 77–99.
- [44] L. Cheng, C. Jin, W. Lv, Q. Ding, and X. Han, Developing a highly stable PLGA-mPEG nanoparticle loaded with cisplatin for chemotherapy of ovarian cancer, *PLoS One*, 6 (2011) 1–9.
- [45] R. B. Weiss and M. C. Christian, New Cisplatin Analogues in Development: A Review, *Drugs*, 46 (1993) 360–377.
- [46] M. B. T. Abrama, R. Kacimia, L. Bejjita, M. N. Bennanib, DFT/TDDFT studies of the structural, electronic, NBO and non-linear optical properties of triphenylamine functionalized tetrathiafulvalene, *Turkish Comput. Theor. Chem.*, 2 (2018) 36–48.
- [47] M. J. Islam, A. Kumer, and M. W. Khan, The theoretical study of anticancer rhodium complexes and methyl groups effect on ligands in chemical reactivity, global descriptors, ADMET by DFT study, *Turkish Comput. Theor. Chem.*, 5 (2021) 1–13.
- [48] A. K. N. Yuksel and M. F. Fellah, Metal-Porphyrin Complexes: A DFT Study of Hydrogen Adsorption and Storage, *Turkish Comput. Theor. Chem.*, 6 (2022) 38–48.
- [49] J. S. Al-Otaibi, Y. S. Mary, R. Thomas, and S. Kaya, Detailed Electronic Structure, Physico-Chemical Properties, Excited State Properties, Virtual Bioactivity Screening and SERS Analysis of Three Guanine Based Antiviral Drugs Valacyclovir HCl Hydrate, Acyclovir and Ganciclovir, *Polycycl. Aromat. Compd.*, 42 (2022) 1260–1270.